Article

Effect of Bergamot Leaves (*Citrus bergamia*) in the Crosstalk between Adipose Tissue and Liver of Diet-Induced Obese Rats

Juliana Silva Siqueira [1,*], Erika Tiemi Nakandakare-Maia [1], Taynara Aparecida Vieira [1], Thiago Luiz Novaga Palacio [1], Núbia Alves Grandini [1], Matheus Antônio Filiol Belin [1], Gisele Alborghetti Nai [2], Fernando Moreto [1], Alessandra Altomare [3], Giovanna Baron [3], Giancarlo Aldini [3], Fabiane Valentini Francisqueti-Ferron [1,4] and Camila Renata Correa [1]

[1] Botucatu Medical School, Sao Paulo State University (Unesp), Botucatu 18618-687, Brazil; fernando.moreto@unesp.br (F.M.)
[2] Department of Pathology, University of Western São Paulo (Unoeste), Presidente Prudente 19061-395, Brazil; patologia@unoeste.br
[3] Department of Pharmaceutical Sciences, University of Milan, 20133 Milan, Italy; giancarlo.aldini@unimi.it (G.A.)
[4] Integrated Colleges of Bauru (FIB), Bauru 17056-100, Brazil
[*] Correspondence: juliana.siqueira@unesp.br

Abstract: The excessive consumption of diets rich in sugar and fat is associated with metabolic manifestations involving adipose tissue and the liver. Bergamot, due to its antioxidant and anti-inflammatory properties, has been used to treat metabolic disorders. This work aimed to verify the effect of Bergamot leaves extract (BLE) on the crosstalk in the adipose tissue–liver axis of obese rats. For 20 weeks, Wistar rats were distributed into two groups: control (Control) and high sugar–fat (HSF) diet groups. Afterwards, the animals were redistributed into three groups for 10 weeks: control diet + vehicle (Control, *n* = 08), HSF + vehicle (HSF, *n* = 08), and HSF + BLE (HSF + BLE, *n* = 08). The BLE was carried out daily by gavage (50 mg/kg). The HSF group presented obesity, hyperglycemia, hypertriglyceridemia, insulin resistance, hepatic microvesicular steatosis, higher inflammation and oxidative stress in the liver and adipose tissue. In comparison to the HSF group, HSF + BLE animals showed protection by reducing the triglyceride levels, insulin resistance, inflammation and oxidative stress in hepatic and adipose tissues. BLE acted on the inflammation and oxidative stress in the adipose tissue–liver axis in obese rats when compared to the HSF group, which may have reflected on the improvement of insulin resistance and dyslipidemia.

Keywords: inflammation; leaf; oxidative stress; western diet; bioactive compound

1. Introduction

Inflammation and oxidative stress are pathogenic pillars for the emergence of various diseases, including obesity [1]. In an obesogenic condition, the presence of a chronic pro-inflammatory and oxidant scenario leads to metabolic complications, such as insulin resistance, which acts as an etiological trigger for comorbidities. Insulin resistance, in addition to triggering diabetes and cardiovascular disease, can affect the adipose tissue–liver axis, contributing to the evolution of nonalcoholic fatty liver disease (NAFLD) [2]. Under physiological conditions, there is a crosstalk between the liver and the adipose tissue to maintain the metabolic homeostasis. In a positive energy balance condition, this communication is impaired, contributing to metabolic derangement and dysfunction [3]. Adipose tissue (AT) becomes hypertrophied, leading to an increase in tissue mass, which is defined as obesity. As a consequence, increased oxygen consumption is triggered in AT, which, in addition to favoring oxidative stress, reduces its supply to the tissue, resulting in necrosis [4]. These two conditions favor the recruitment of inflammatory cells from the circulation, releasing inflammatory cytokines and chemokines, such as alpha tumor necrosis

factor (TNF-α), interleukin-6 (IL-6) and monocyte chemoattractant protein-1 (MCP-1), among others [5].

Specifically, TNF-α and IL-6 impair the responsiveness of adipose tissue to insulin, interfering with the ability of adipocytes to capture fatty acids from the circulation, favoring the hydrolysis of intracellular triglycerides and releasing more fatty acids into the circulation [6,7]. Given this scenario, circulating fatty acids are stored in hepatocytes as a result of dysfunctional adipose tissue that initiates a steatosis process in the liver. When this fat supply is not controlled, the immune cells can also infiltrate the liver, contributing even more to a low-grade chronic intrahepatic inflammatory process as well as the imbalance of the redox system, resulting in oxidative stress. When prolonged, these two pathogenic pillars contribute to fibrogenesis that can result in cirrhosis [8,9].

On the other hand, lifestyle changes with an emphasis on healthy eating and the addition of bioactive compounds, found in vegetables and fruits, rich in polyphenols, act beneficially by reducing inflammation and oxidative stress generated by diets rich in sugars and fats [10]. Therefore, investigating the different dietary interventions and exploring the different types of foods to serve as therapeutic strategies to combat inflammation and oxidative stress can help prevent or treat their consequences.

Bergamot (*Citrus bergamia*), similar to other citrus fruits, is rich in flavonoids and performs potential antioxidant and anti-inflammatory activity with beneficial properties in metabolic complications due to its hypolipidemic and hypoglycemic effects [11,12]. The literature reports that flavonoids are able to modulate carbohydrate and lipid metabolism, improving obesity-related metabolic disorders such as hyperglycemia, insulin resistance, oxidative stress and inflammatory processes [13]. As some plants have a phenolic composition of the leaves that is similar to, or superior than, the fruit [14], Baron et al. (2021) conducted a study that revealed that Bergamot leaves have increased levels of polyphenols, suggesting that the leaves can promote the same or higher beneficial actions found in the fruit [15].

Furthermore, the principal flavonoid and nonflavonoid components found in Bergamot leaves have already been discussed. Among its constituents, naringin and hesperidin play an important role in inflammation, oxidative stress and lipid metabolism regulators, acting on fat synthesis, storage and utilization through different pathways that promote improvement in liver dysfunction [16,17]. In addition, neohesperidin is able to improve insulin sensitivity and regulate fat accumulation mediated by adenosine monophosphate-activated protein kinase (AMPK) signaling [16]. Furthermore, the beneficial effect of apigenin on lipid metabolism and hepatic dysfunction was attributed to its capacity to up-regulate genes involved in fatty acid oxidation, oxidative phosphorylation and cholesterol homeostasis [18]. In addition, the presence of HMG derivatives on the Bergamot leaves contributes to cholesterol-lowering effects [12,15].

It has already been described by our group the anti-inflammatory and antioxidant effect of Bergamot leaves in an in vitro model and also the Bergamot leaves' extract potential to attenuate insulin resistance [19]. However, there are still no studies that correlate this effect with the adipose tissue–liver axis in an experimental model of obesity. Once obesity triggers inflammation and oxidative stress in adipose tissue, resulting in metabolic disorders, the aim of this work was to verify the effect of BLE on the crosstalk in the adipose tissue–liver axis of obese rats.

2. Materials and Methods

2.1. Experimental Protocol and Group Characterization

The Animal Ethics Committee (271/2021) approved the experiments and procedures, which were conducted in compliance with the National Institute of Health's Guide for the Care and Use of Laboratory Animals. Male Wistar rats (±180 g) were maintained in a room with a controlled environment (22 °C $\pm$ 3 °C; 12 h light–dark cycle and relative humidity of 60 $\pm$ 5%) and randomly allocated among 2 experimental groups ad libitum receiving a control diet (Control, $n = 10$) and high sugar–fat diet + 25% of sucrose on the drinking water

(HSF, *n* = 20) for 20 weeks. The diets' compositions followed the model already established and previously published [20].

In the 20th week, when hypertriglyceridemia (C: 93.0 ± 38.2 vs. HSF: 139.5 ± 69.7, *p* < 0.001) and insulin resistance (C: 3.8 ± 0.9 vs. HSF: 5.5 ± 1.3, *p* < 0.001) were detected in the HSF group, a separation point (SP) was adopted once animals exposed to different diet models did not always present the expected response [19,21]. After that, the control and HSF groups of animals, above and below the SP, respectively, were excluded from the experiment.

After this period, the animals were randomly redistributed into 3 experimental groups: Control diet + vehicle (Control, *n* = 08) high sugar–fat diet + 25% of sucrose on the drinking water + vehicle (HSF, *n* = 08), high sugar–fat diet + 25% of sucrose on the drinking water + Bergamot leaves extract (HSF + BLE, *n* = 08) for 10 weeks.

In the 30th week, after 8 h of fasting, the animals were anesthetized with thiopental (120 mg/kg/IP) and the caudal, interdigital, foot and eyelid reflexes were checked to proceed with decapitation and tissue collection. The blood, adipose and hepatic tissues of each animal were collected.

2.2. Bergamot Leaves Extract (BLE)

The dried extract of the BLE was produced at the H&AD (Herbal & Antioxidant Derivatives S.r.l.) farm located in Località Chiusi, 89032 Bianco (RC), Italy (www.head-sa. com, accessed on 8 May 2023). A previously published work demonstrates details about the extraction procedure, formulation and dose [19]. The BLE was given daily by gavage at a dose of 50 mg/kg of body weight. The vehicle groups received filtered water by gavage.

2.3. Analysis of Nutrition and Metabolism

The nutritional profile was assessed considering the individual dietary intake, calorie intake and the final body weight. The consumption of the chow and water of each animal were measured weekly, and the caloric intake was determined by multiplying the energy value of each diet (g × Kcal). The epididymal, visceral and retroperitoneal fat deposits were dissected during euthanasia and used as a sign of obesity using the adiposity index determination, following the formula: Adiposity index = [(Epididymal fat + Visceral fat + Retroperitoneal fat)/final body weight] × 100 [21,22].

The systolic blood pressure was assessed by tail-cuff plethysmography in the conscious rats using a NarcoBioSystems® Electro-Sphygmomanometer (International Biomedical, Austin, TX, USA). The animals were individually heated in a wooden box at 40 °C for 5 min for the purpose of induce vasodilation of caudal artery [23]. The records were collected using a Gould RS 3200 polygraph (Gould Instrumental Valley View, OH, USA). For each animal, the average of three pressure values was obtained.

Before euthanasia, the glucose levels (mg/dL) were evaluated through blood collection and measured by pouring a drop of blood to the edge of the test strip, using a glucometer (Accu-Chek Performa; Roche Diagnostics, Indianapolis, IN, USA). The plasma was centrifuged (1500 rpm for 10 min) and aliquoted during euthanasia for biochemical analysis (plasmatic levels triglycerides, insulin and insulin resistance). The triglyceride levels (mg/dL) were measured with an automatic enzymatic analyzer system (Chemistry Analyzer BS-200, Mindray Medical International Limited, Shenzhen, China). The insulin level was measured using the enzyme-linked immunosorbent assay (ELISA) method using commercial kits (Rat INS ELISA Kit, E-EL-R3034, Elabscience Biotechnology Inc., Houston, TX, USA) and the reading was carried out in a Spectramax 190 microplate spectrophotometer (Molecular Devices®, Sunnyvale, CA, USA). As an insulin resistance index, the homeostatic model of insulin resistance (HOMA-IR) was used, according to the formula: HOMA-IR = (fasting glucose (mmol/L) × fasting insulin (μU/mL))/22.5 [24].

2.4. Hepatic Lipidosis

The presence of microvesicular lipidosis was evaluated through the analysis of histological slides of the hepatic tissue. After euthanasia and hepatic left lobe collection,

the fraction of liver tissue was maintained for 24 h in 4% paraformaldehyde with 0.1 M phosphate buffer (pH = 7.4). After this period, the tissue was transferred to ethyl alcohol until fixed in paraffin. Histological sections were obtained from the paraffinized block, fixed on a slide and stained with hematoxylin and eosin (H&E). The slides were analyzed by a trained pathologist for the presence of microvesicular lipidosis based on the percentage of affected hepatocytes per observed field (10 fields). Fields were scored as 0 (none to 5% affected), 1 (6–25%), 2 (26–50%), 3 (51–75% affected) and 4 (75–100%) and the mean of the fields were calculated to each animal; adapted from Moreto et al. (2021) [25].

2.5. Hepatic Function

The aspartate aminotransferase (AST) and alanine aminotransferase (ALT) plasmatic levels were measured by an enzymatic-colorimetric method using an automated device (Technicon, RA-XTTM System, Global Medical Instrumentation, Minneapolis, MN, USA), using CELM kits®, Barueri, São Paulo, Brazil. The ratio between AST and ALT (Ritis ratio) marked the progression of liver impairment [26].

2.6. Adipose and Hepatic Tissues Preparation for Analysis

Briefly, 200 mg of epididymal adipose tissue and 100 mg of hepatic tissue were homogenized in 1 mL of Phosphate-buffered saline solution (PBS, pH 7.4), for inflammatory parameter analysis and oxidative stress markers, or Potassium chloride solution (KCl, 1.15%) for antioxidant enzymes, using ULTRA-TURRAX® T25 basic IKA® Werke Staufen/Germany, and centrifuged at 1500 rpm at 4 °C for 10 min. The intermediate layers in the adipose tissue samples and hepatic supernatant were collected to perform the analysis.

2.7. Inflammatory Parameters

The pro-inflammatory marker, TNF-α and IL-6, were assessed using the ELISA method using commercial kits (Rat TNF-alpha DuoSet ELISA, DY510; Rat IL-6 DuoSet ELISA, DY506; R&D System, Minneapolis, MN, USA).

2.8. Oxidative Stress Markers

As previously established, the malondialdehyde (MDA) levels were utilized to estimate the lipid peroxidation [27]. Briefly, 0.33 g of thiobarbituric acid (TBA) 0.67% was added to a solution of 7.5 g of tricloroacetic acid, 6.25 mL of hydrocloric acid and deionized water to complete 50 mL of working solution. In total, 200 uL of each adipose and hepatic tissue sample was added to 500 uL of the solution, worked in test tubes and centrifuged at 1500 rpm for 10 min. After that, the supernatant was collected and heated for 45 min in a water bath at 100 °C. The Spectra Max 190 microplate reader (Molecular Devices, Sunnyvale, CA, USA) was used to conduct the reading at 532 nm and 600 nm. The MDA concentration was obtained by the molar extinction coefficient (1.56×10^5 M^{-1} cm^{-1}) and the difference of the absorbance of the samples and the final results were expressed in nmol/mg protein.

The DNPH (2,4-dinitrophenylhydrazine) technique was used to detect carbonylated proteins [28]. In total, 100 uL of sample was mixed with 100 uL of DNPH 10 nM and incubated for 10 min. The sample + DNPH wells were then treated with 50 uL of NaOH 6 M and incubated for an additional 10 min. The reading was performed at 450 nm and the results calculated with a molar extinction coefficient (22.000 M^{-1} cm^{-1}) of DNPH and expressed as nmol/mg protein.

Based on the suppression of the superoxide radical interaction with pyrogallol by spectrophotometry at 420 nm, the superoxide dismutase (SOD) activity was determined. The results were represented in U/mg protein/minute. One unit of SOD activity (U) is defined as the quantity of the enzyme that blocked 50% of pyrogallol autoxidation [29].

The catalase (CAT) activity was determined by the decrease in hydrogen peroxide (30%) levels. The dissociation of hydrogen peroxide in the reaction mixture was measured

spectrophotometrically at 240 nm every 20 s for 2 min, and the results were expressed as pmol/mg protein/minute [30].

The FRAP (Ferric Reducing Antioxidant Power) assay was adapted, according to the methodology proposed by Benzie and Strain, to determine the antioxidant activity by reducing iron through the reaction between the samples and FRAP reagent (FeCl$_3$ 20 nmol/L, acetate buffer 0.3 mol/L and 2,4,6-Tri(2-pyridyl)-s-triazine 10 mmol/L) presented in uM FeSO$_4$·H$_2$O/ug protein in each tissue [31].

2.9. Statistical Analysis

Data are presented as mean ± standard deviation (SD). The groups were statistically analyzed by one-way ANOVA test with Tukey's post hoc using Sigma Stat for Windows Version 3.5 (Systat Software, Inc., San Jose, CA, USA). A 0.05 *p* value was considered statistically significant. All the graphs were performed using GraphPad Prism software version 9.0 for Mac.

3. Results

3.1. Nutritional and Metabolic Parameters

The nutritional and metabolic parameters at the end of the experimental protocol are presented in Table 1. The HSF diet promoted an increased caloric intake, final body weight, adiposity index, glucose, triglycerides, insulin and HOMA-IR levels and hypertension, confirming the experimental model of obesity and metabolic disorders, which are risk factors for the development of hepatic diseases. In addition, the animals of the HSF + BLE group presented a higher caloric intake, triglycerides, insulin and HOMA-IR levels compared to the Control group. On the other hand, BLE treatment demonstrated effectiveness in attenuating hypertriglyceridemia, hyperinsulinemia and insulin resistance in relation to the HSF group.

Table 1. Nutritional and metabolic parameters in 30 weeks.

	Groups		
	Control	**HSF**	**HSF + BLE**
Caloric Intake (kcal/day)	90.6 ± 5.4	104 ± 8 [#]	102 ± 11 [$]
Final Weight (g)	472 ± 56	586 ± 74 [#]	542 ± 71
Adiposity Index (%)	4.64 ± 1.33	8.60 ± 1.92 [#]	7.11 ± 1.99 [$]
Glucose (mg/dL)	87.2 ± 9.4	99.5 ± 7.5 [#]	90.6 ± 10.8
Triglycerides (mg/dL)	28.4 ± 5.7	95.5 ± 11.1 [#]	60.1 ± 10.7 [$,*]
Insulin (µU/mL)	7.01 ± 2.72	28.05 ± 4.36 [#]	18.82 ± 3.59 [$,*]
HOMA-IR	1.62 ± 0.43	6.90 ± 1.35 [#]	4.22 ± 1.02 [$,*]
Systolic Blood Pressure (mmHg)	114 ± 6	141 ± 7 [#]	144 ± 13 [$]

Data are expressed as mean ± standard deviation. Comparison by one-way ANOVA with Tukey's post hoc. *p* < 0.05 were considered statistically significant. BLE—Bergamot leaves extract. HSF—high sugar–fat diet. HOMA-IR—homeostatic model of insulin resistance. [#] HSF vs. Control; [$] HSF + BLE vs. Control; [*] HSF vs. HSF + BLE.

3.2. Hepatic Function and Microvesicular Lipidosis

The hepatic function and microvesicular lipidosis are presented in Figure 1. The HSF groups (HSF and HSF + BLE) presented increased hepatic microvesicular lipidosis in relation to the Control group (Figure 1D).

No differences were observed in the Ritis ratio between the experimental groups (Figure 2).
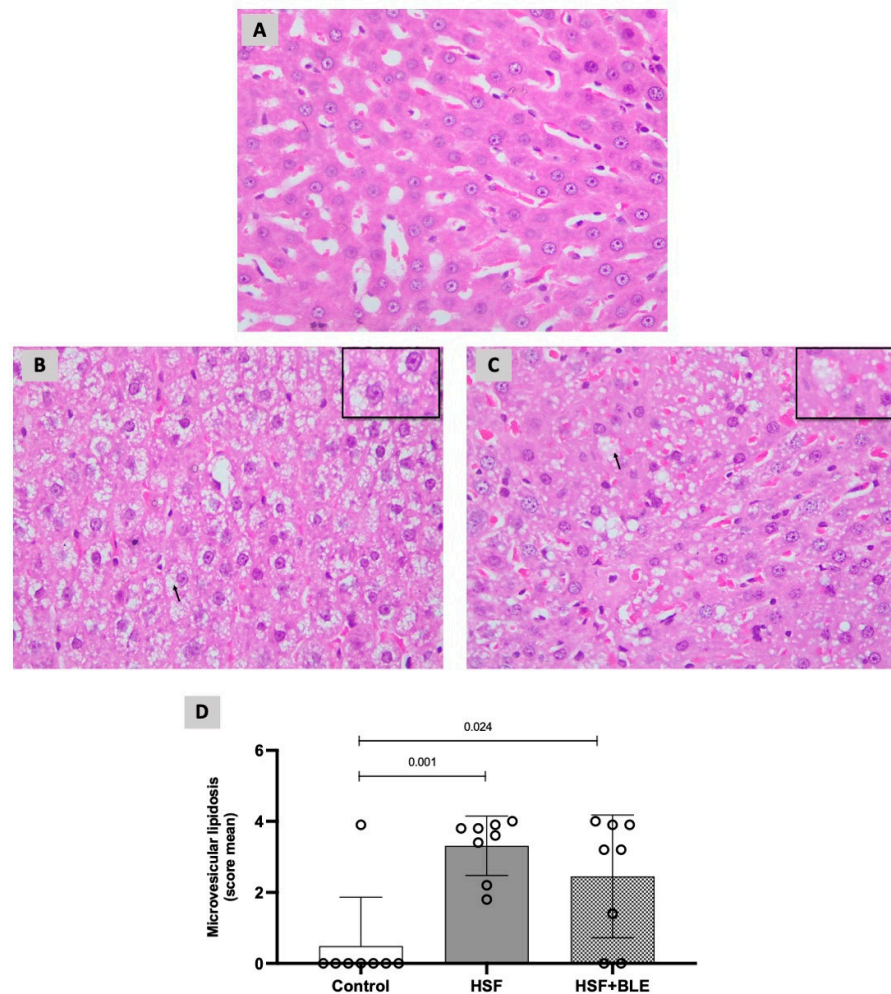
Figure 1. Hepatic microvesicular lipidosis. (**A**) Normal liver parenchyma in the image referring to (**A**) control group. Microvesiculation of the parenchyma of hepatocytes characterizing microgoticular lipidosis in the (**B**) HSF group and (**C**) HSF + BLE. Hematoxylin and eosin, 200× magnification. (**D**) Microvesicular lipidosis (score mean). Data are expressed as mean ± standard deviation. Comparison by one-way ANOVA with Tukey's post hoc. $p < 0.05$. HSF—high sugar–fat diet. BLE—Bergamot leaves extract. The black arrow indicates the presence of microvesicular lipidosis.
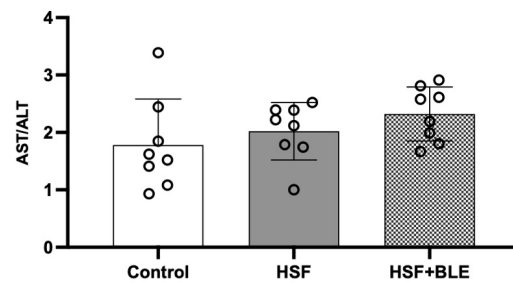
Figure 2. AST/ALT. Data are expressed as mean ± standard deviation. Comparison by one-way ANOVA with Tukey's post hoc. $p < 0.05$. AST—aspartate aminotransferase. ALT—alanine aminotransferase. BLE—Bergamot leaves extract. HSF—high sugar–fat diet.

3.3. RedOx–Inflammatory State in the Adipose Tissue

Figure 3 shows the RedOx–Inflammatory state of AT (adipose tissue) at the conclusion of the experimental protocol. The animals of the HSF group showed increased levels of TNF-α, IL-6, malondialdehyde and protein carbonyl content and reduced levels of FRAP in

relation to the Control group. In addition, the HSF + BLE presented higher levels of protein carbonyl content and CAT enzyme in relation to the Control group. The treatment with BLE promoted an amelioration of pro-inflammatory markers (lower TNF-α and IL-6) and oxidative stress (lower malondialdehyde levels and higher levels of CAT enzyme activity) in relation to the HSF group.
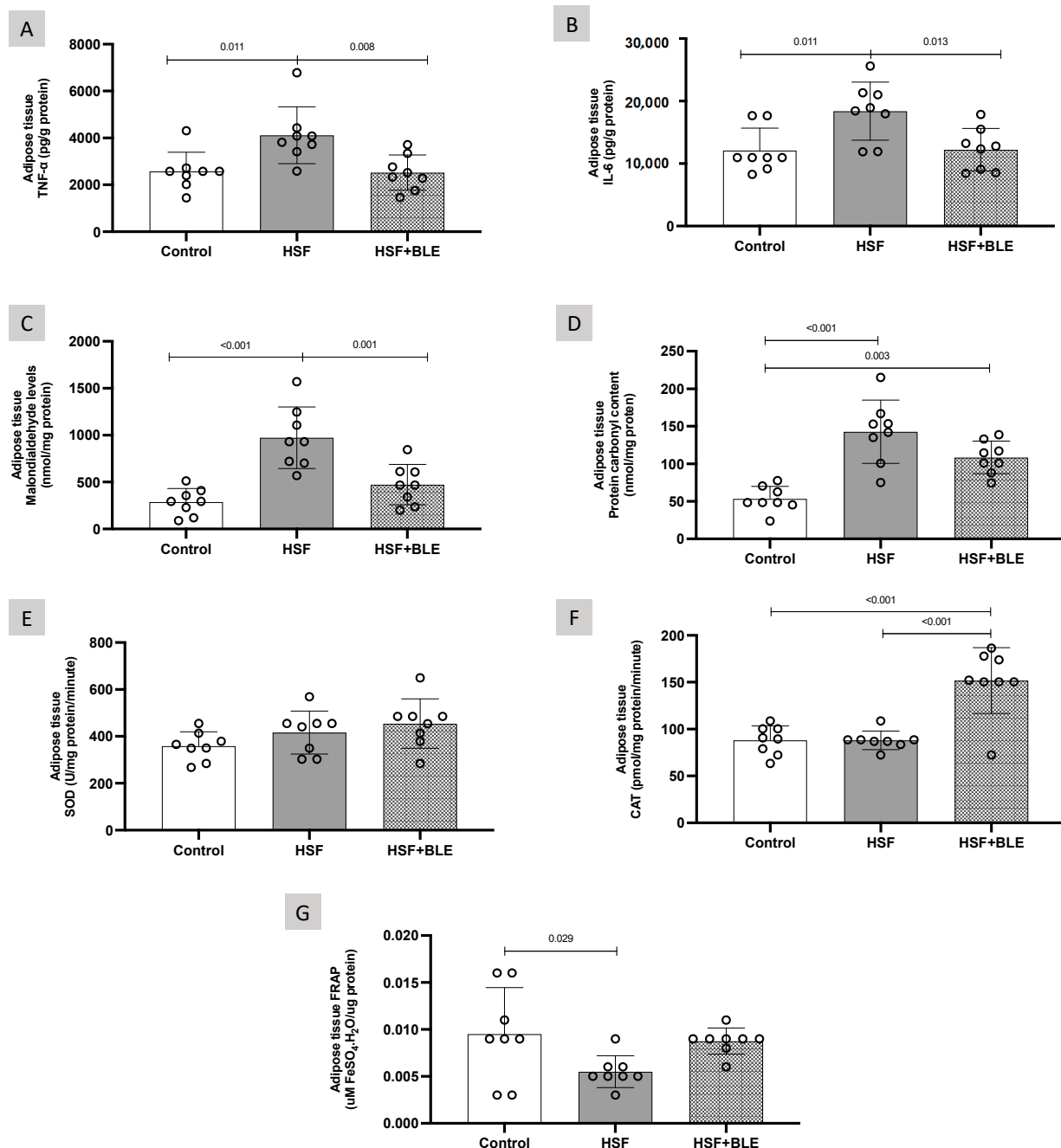

Figure 3. Adipose tissue RedOx–inflammatory state in the 30th week. (**A**) TNF-α (pg/g protein); (**B**) IL-6 (pg/g protein); (**C**) malondialdehyde levels (nmol/mg protein); (**D**) protein carbonyl content (nmol/mg protein); (**E**) SOD (U/mg protein/min); (**F**) CAT (pmol/mg protein/minute); (**G**) FRAP (uM FeSO$_4$·H$_2$O/ug protein). Data are expressed as mean ± standard deviation. Comparison by one-way ANOVA with Tukey's post hoc. $p < 0.05$. TNF-α—tumor necrosis factor alpha. IL-6—interleukin-6. SOD—superoxide dismutase enzyme activity. CAT—catalase enzyme activity. FRAP—ferric reducing ability of plasma. BLE—Bergamot leaves extract. HSF—high sugar–fat diet.

3.4. RedOx–Inflammatory State in the Hepatic Tissue

Figure 4 shows the hepatic RedOx–Inflammatory state at the end of the experimental protocol. The animals of the HSF group showed higher levels of TNF-α, IL-6, malondialdehyde and protein carbonyl content and reduced levels of SOD and CAT enzyme activity and FRAP in relation to the Control group. The treatment with BLE promoted an amelioration of inflammation (lower TNF-α) and oxidative stress (lower malondialdehyde and protein carbonyl content levels and higher levels of CAT enzyme activity and FRAP) markers in relation to the HSF group.
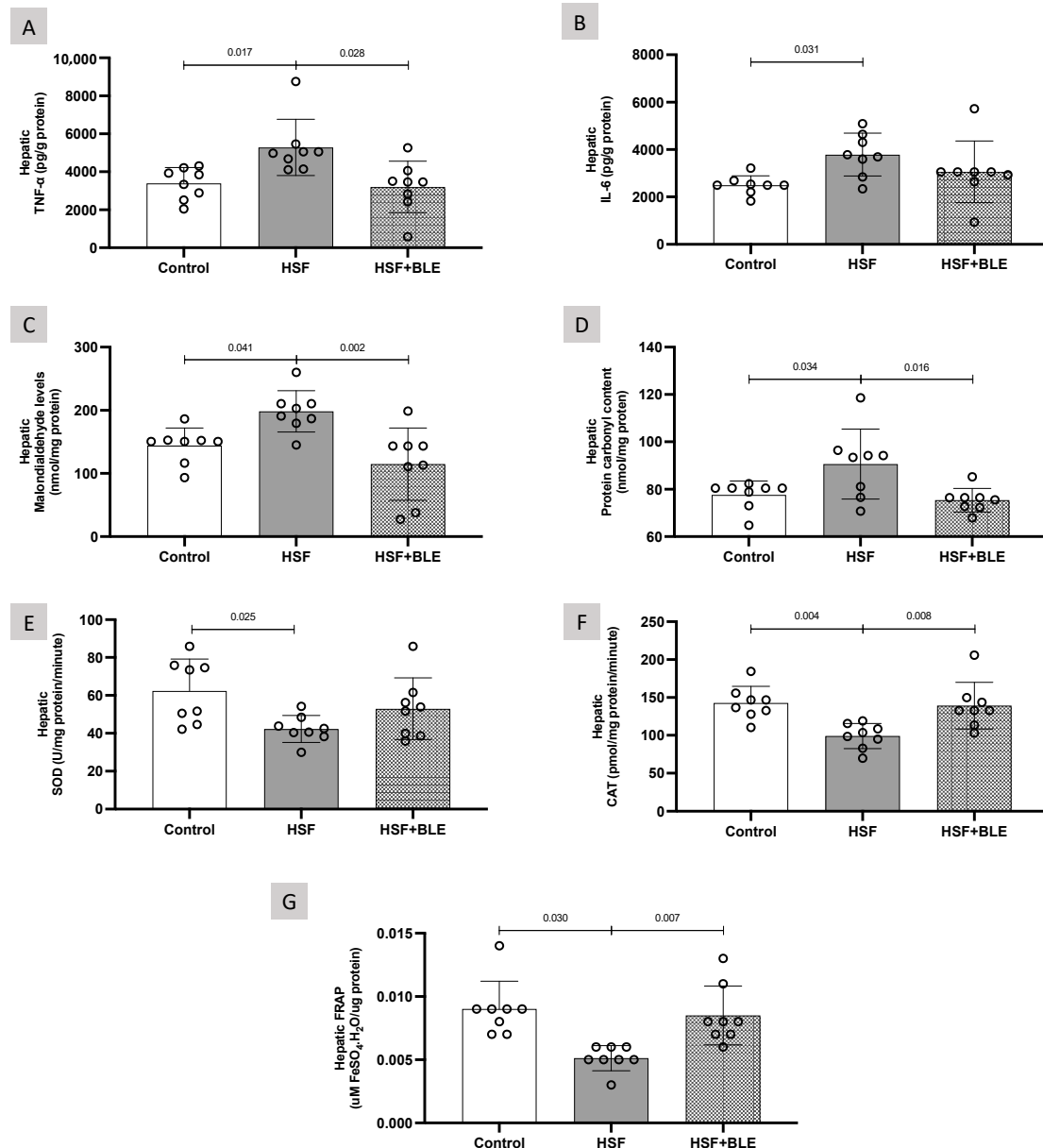
Figure 4. Hepatic RedOx–Inflammatory state in the 30th week. (**A**) TNF-α (pg/g protein); (**B**) IL-6 (pg/g protein); (**C**) malondialdehyde levels (nmol/mg protein); (**D**) protein carbonyl content (nmol/mg protein); (**E**) SOD (U/mg protein/min); (**F**) CAT (pmol/mg protein/minute); (**G**) FRAP (uM FeSO$_4$·H$_2$O/ug protein). Data are expressed as mean ± standard deviation. Comparison by one-way ANOVA with Tukey's post-hoc. $p < 0.05$. TNF-α—tumor necrosis factor alpha. IL-6—interleukin-6. SOD—superoxide dismutase enzyme activity. CAT—catalase enzyme activity. FRAP—ferric reducing ability of plasma. BLE—Bergamot leaves extract. HSF—high sugar–fat diet.

3.5. Correlation between Nutritional, Metabolic and Liver and Adipose Tissue RedOx–Inflammatory State

Figure 5 presents the Pearson correlation among variables. It is possible to note that insulin resistance, represented by the HOMA calculation, presented a significant positive association with microvesicular lipidosis, triglycerides, the adiposity index, inflammation and oxidative stress, which may point to a dysfunction of the adipose tissue in storing fat. In addition, it is possible to observe an association between the proinflammatory cytokines and oxidative stress markers in both tissues and a significant negative association in relation to the antioxidant capacity in adipose tissue and liver.
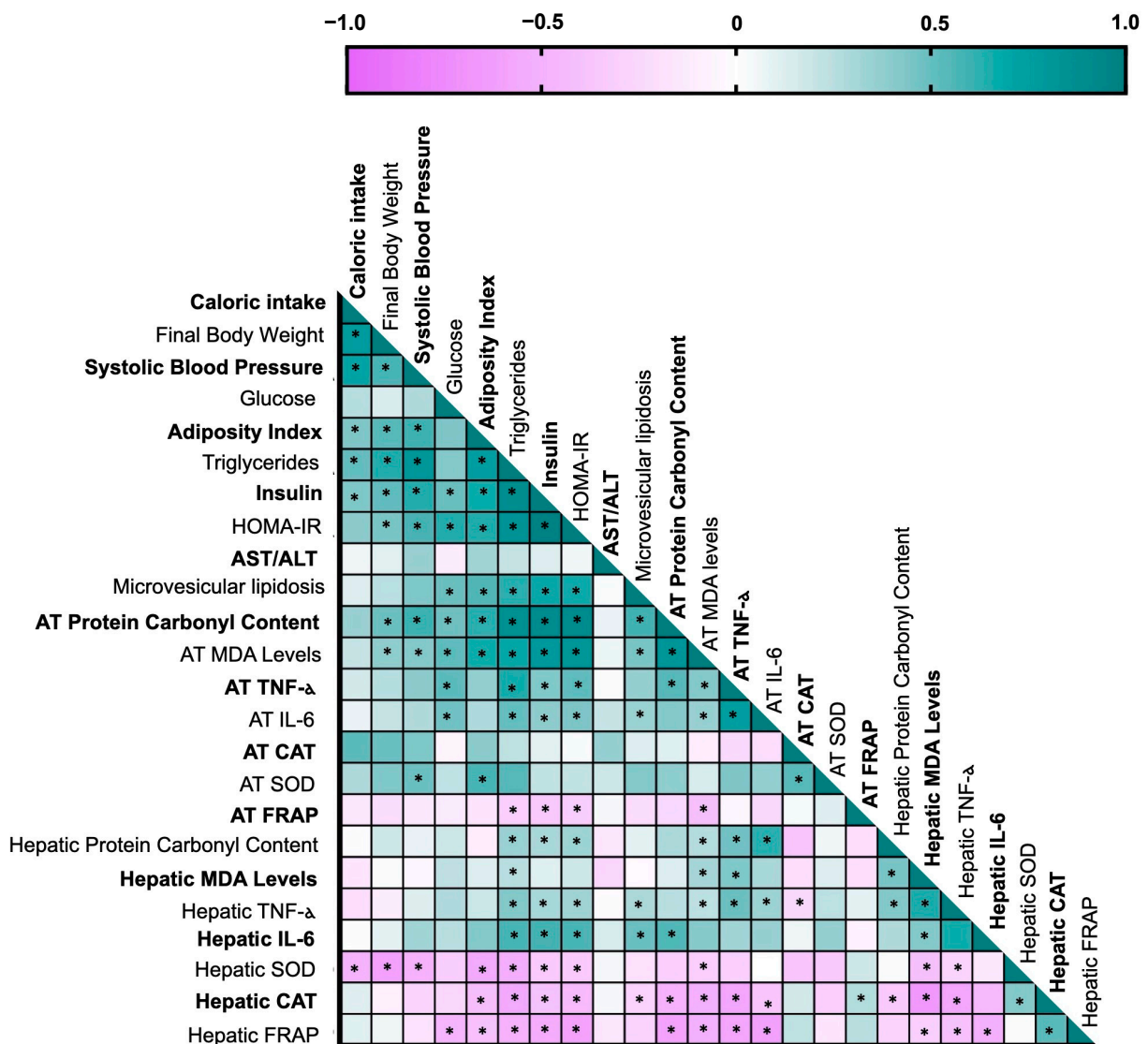

Figure 5. Correlation matrix among the variables. Positive correlations are presented in green and negative correlations are presented in purple. The color intensity is proportional to the correlation coefficients. * Indicates correlations with $p < 0.05$. AT—adipose tissue. HOMA-IR—homeostatic model of insulin resistance. MDA—malondialdehyde. TNF-α—tumor necrosis factor alpha. IL-6—interleukin-6. SOD—superoxide dismutase enzyme activity. CAT—catalase enzyme activity. FRAP—ferric reducing ability of plasma.

4. Discussion

This study aimed to confirm the impact of Bergamot leaves on the interaction between the adipose tissue and liver in obese rats. The animals that consumed the HSF diet (HSF and HSF + BLE groups) presented obesity, hypertension, hypertriglyceridemia and insulin resistance when compared to the animals that consumed the control diet. These results demonstrated that the diet promoted the expected effects, once in a positive energy balance the excess of nutrients contributes to the metabolic derangement observed in this study due to AT impairment as a consequence of its excessive expansion [3,32].

Although physiologically necessary, the adipose tissue has an expansion limit that, once reached, impairs the storage of excess energy in adipocytes, making AT severely dysfunctional, contributing to metabolic damage such as inflammation, alterations in the secretion of adipokines, hypoxia, fibrosis and mitochondrial dysfunction with a consequent increase in ROS production [4,33]. Confirming, the HSF group presented increased levels of pro-inflammatory cytokines, oxidative stress markers and reduced antioxidant activity in the adipose tissue in relation to the control group.

The liver is one of the obesity target organs, responsible for body homeostasis maintenance. Among its functions, it orchestrates the energy metabolism, acting on carbohydrate and lipid metabolism [34,35]. The high consumption of diets rich in simple sugars and saturated fats is associated with the imbalance between the production and degradation of dietary fatty acids, contributing to the accumulation of hepatic lipids [9,36]. These conditions contribute to an increased flow of hepatic free fatty acids (FFAs) and the accumulation of triglycerides (TG) through de novo lipogenesis and lipolysis due to the insulin resistance scenario, leading to an increase in the liver's production of pro-inflammatory cytokines and oxidative stress, which supports the association between hepatic diseases and obesity [37]. Therefore, our results corroborate the literature once the HSF group presented hepatic microvesicular lipidosis, increased expression of TNF-α, IL-6, MDA, protein carbonyl content and reduced antioxidant activity.

Contrarily, the eating habit of consuming fruits and vegetables, rich in bioactive compounds, is a therapeutic strategy against the metabolic disorders resulting from obesity. The synergistic interaction between the compounds of the extract can act to potentiate the beneficial effects when compared to their isolated effects [38,39]. A study combining naringin and vitamin C, flavonoid and nonflavonoid components of bergamot extract, showed an improvement in the antihyperglycemic and antioxidant effects in an experimental model of diabetes [40]. In addition, when combined, hesperitin and hesperidin promote lipid-lowering activity due to their actions on glucose and lipid metabolism [41].

That said, the HSF + BLE animals showed decreased levels of lipids, insulin levels and insulin resistance compared to the HSF group. Although the mechanisms of BLE action are not yet fully elucidated, these data are in accordance with studies with bergamot fruit, which demonstrate that the hypolipidemic effect of Bergamot are associated with the modulation of the activity of enzymes responsible for cholesterol esterification and lipid traffic [11,42]. This result may be attributed in part to the greater fecal excretion of sterols in rats receiving the bergamot extract and to the composition of flavonoids present in the extract, in particular naringin and neohesperidin, which experience the activity of enzymes involved in the formation of diacylglycerol in a hyperglycemic context and also in acting on lipid availability for lipoprotein assembly through association with Apolipoprotein B, an integral part in the transport of lipids to tissues [12,43]. In addition, Bergamot fruit seems to act directly at the MAPK pathway, an important regulator of glucose and FFA metabolism [44,45]. Particularly, in the fatty liver disease, the fruit induced modulation of JNK/p38 MAPKs, a protective mechanism responsible for insulin sensitivity amelioration [45], highlighting the leaves' potential as a possible adjuvant in the treatment of metabolic diseases.

The antioxidant and anti-inflammatory activity of BLE were observed through the reduction in pro-inflammatory cytokines and oxidant markers and the improvement of the antioxidant capacity in the adipose and liver tissues. Published works show that

BLE performed an anti-inflammatory action via the inhibition of the activation of nuclear transcription factor kappa-B (NF-kB) and an antioxidant action from the Nuclear factor erythroid 2-related factor 2 (Nrf2) pathway [15,19]. Apigenin and luteolin, two of the main flavonoids present in the Bergamot leaf, are able to promote an anti-inflammatory and antioxidant effect through the modulation of different pathways [46]. It is known that the compounds are able to inactivate NF-kB and enhance the expression of antioxidant enzymes such as SOD and CAT [47]. In addition, rats with nonalcoholic steatohepatitis (NASH) induced by a cafeteria diet presented lower levels of IL-6 and increased anti-inflammatory mediators expression when supplemented with the polyphenolic fraction of bergamot [48]. These effects can be attributed to the flavanone and flavone glycosides, as well as to their aglycones composition [15]. The amelioration of these parameters acts on glucose uptake improving insulin sensitivity [49]. That said, it is possible to observe a positive correlation between the RedOx–Inflammatory parameters in the adipose and liver tissues with insulin sensitivity in Figure 5.

Although Bergamot leaves' extract has not been tested in human clinical trials, this study provides a starting point for future research involving the specific pathways of BLE, a promising candidate for the prevention and treatment of conditions related to the adipose–liver tissue axis.

5. Conclusions

In summary, this study showed that Bergamot leaves acted on the inflammation and oxidative stress in the adipose tissue–liver axis in obese rats, which may have reflected on the improvement of insulin resistance and dyslipidemia.

References

1. Monserrat-Mesquida, M.; Quetglas-Llabrés, M.; Capó, X.; Bouzas, C.; Mateos, D.; Pons, A.; Tur, J.A.; Sureda, A. Metabolic Syndrome Is Associated with Oxidative Stress and Proinflammatory State. *Antioxidants* **2020**, *9*, 236. [CrossRef] [PubMed]
2. Polyzos, S.A.; Kountouras, J.; Mantzoros, C.S. Obesity and Nonalcoholic Fatty Liver Disease: From Pathophysiology to Therapeutics. *Metabolism* **2019**, *92*, 82–97. [CrossRef] [PubMed]
3. Duwaerts, C.C.; Maher, J.J. Macronutrients and the Adipose-Liver Axis in Obesity and Fatty Liver. *Cell. Mol. Gastroenterol. Hepatol.* **2019**, *7*, 749–761. [CrossRef] [PubMed]
4. Longo, M.; Zatterale, F.; Naderi, J.; Parrillo, L.; Formisano, P.; Raciti, G.A.; Beguinot, F.; Miele, C. Adipose Tissue Dysfunction as Determinant of Obesity-Associated Metabolic Complications. *Int. J. Mol. Sci.* **2019**, *20*, 2358. [CrossRef]
5. Francisqueti, F.V.; do Nascimento, A.F.; Correa, C.R. Obesidade, Inflamação e Complicações Metabólicas. *Nutrire* **2015**, *40*, 81–89. [CrossRef]

6. Kern, P.A.; Ranganathan, S.; Li, C.; Wood, L.; Ranganathan, G. Adipose Tissue Tumor Necrosis Factor and Interleukin-6 Expression in Human Obesity and Insulin Resistance. *Am. J. Physiol. Metab.* **2001**, *280*, E745–E751. [CrossRef]
7. Hotamisligil, G.S.; Shargill, N.S.; Spiegelman, B.M. Adipose Expression of Tumor Necrosis Factor-α: Direct Role in Obesity-Linked Insulin Resistance. *Science* **1993**, *259*, 87–91. [CrossRef]
8. Buzzetti, E.; Pinzani, M.; Tsochatzis, E.A. The Multiple-Hit Pathogenesis of Non-Alcoholic Fatty Liver Disease (NAFLD). *Metabolism* **2016**, *65*, 1038–1048. [CrossRef]
9. Chen, Z.; Tian, R.; She, Z.; Cai, J.; Li, H. Role of Oxidative Stress in the Pathogenesis of Nonalcoholic Fatty Liver Disease. *Free Radic. Biol. Med.* **2020**, *152*, 116–141. [CrossRef]
10. Teodoro, A.J. Bioactive Compounds of Food: Their Role in the Prevention and Treatment of Diseases. *Oxid. Med. Cell. Longev.* **2019**, *2019*, 3765986. [CrossRef]
11. Musolino, V.; Gliozzi, M.; Nucera, S.; Carresi, C.; Maiuolo, J.; Mollace, R.; Paone, S.; Bosco, F.; Scarano, F.; Scicchitano, M.; et al. The Effect of Bergamot Polyphenolic Fraction on Lipid Transfer Protein System and Vascular Oxidative Stress in a Rat Model of Hyperlipemia. *Lipids Health Dis.* **2019**, *18*, 115. [CrossRef] [PubMed]
12. Mollace, V.; Sacco, I.; Janda, E.; Malara, C.; Ventrice, D.; Colica, C.; Visalli, V.; Muscoli, S.; Ragusa, S.; Muscoli, C.; et al. Hypolipemic and Hypoglycaemic Activity of Bergamot Polyphenols: From Animal Models to Human Studies. *Fitoterapia* **2011**, *82*, 309–316. [CrossRef] [PubMed]
13. Ginwala, R.; Bhavsar, R.; Chigbu, D.I.; Jain, P.; Khan, Z.K. Potential Role of Flavonoids in Treating Chronic Inflammatory Diseases with a Special Focus on the Anti-Inflammatory Activity of Apigenin. *Antioxidants* **2019**, *8*, 35. [CrossRef] [PubMed]
14. Ferlemi, A.V.; Lamari, F.N. Berry Leaves: An Alternative Source of Bioactive Natural Products of Nutritional and Medicinal Value. *Antioxidants* **2016**, *5*, 17. [CrossRef] [PubMed]
15. Baron, G.; Altomare, A.; Mol, M.; Garcia, J.L.; Correa, C.; Raucci, A.; Mancinelli, L.; Mazzotta, S.; Fumagalli, L.; Trunfio, G.; et al. Analytical Profile and Antioxidant and Anti-Inflammatory Activities of the Enriched Polyphenol Fractions Isolated from Bergamot Fruit and Leave. *Antioxidants* **2021**, *10*, 141. [CrossRef]
16. Lu, K.; Yip, Y.M. Therapeutic Potential of Bioactive Flavonoids from Citrus Fruit Peels toward Obesity and Diabetes Mellitus. *Futur. Pharmacol.* **2023**, *3*, 14–37. [CrossRef]
17. Han, H.-Y.; Lee, S.-K.; Choi, B.-K.; Lee, D.-R.; Lee, H.J.; Kim, T.-W. Preventive Effect of Citrus Aurantium Peel Extract on High-Fat Diet-Induced Non-Alcoholic Fatty Liver in Mice. *Biol. Pharm. Bull.* **2019**, *42*, 255–260. [CrossRef]
18. Jung, U.; Cho, Y.-Y.; Choi, M.-S. Apigenin Ameliorates Dyslipidemia, Hepatic Steatosis and Insulin Resistance by Modulating Metabolic and Transcriptional Profiles in the Liver of High-Fat Diet-Induced Obese Mice. *Nutrients* **2016**, *8*, 305. [CrossRef]
19. Siqueira, J.S.; Vieira, T.A.; Nakandakare-Maia, E.T.; Palacio, T.L.N.; Sarzi, F.; Garcia, J.L.; de Paula, B.H.; Bazan, S.G.Z.; Baron, G.; Tucci, L.; et al. Bergamot Leaf Extract Treats Cardiorenal Metabolic Syndrome and Associated Pathophysiological Factors in Rats Fed with a High Sugar Fat Diet. *Mol. Cell. Endocrinol.* **2022**, *556*, 111721. [CrossRef]
20. Francisqueti, F.; Minatel, I.; Ferron, A.; Bazan, S.; Silva, V.; Garcia, J.; de Campos, D.; Ferreira, A.; Moreto, F.; Cicogna, A.; et al. Effect of Gamma-Oryzanol as Therapeutic Agent to Prevent Cardiorenal Metabolic Syndrome in Animals Submitted to High Sugar-Fat Diet. *Nutrients* **2017**, *9*, 1299. [CrossRef]
21. Nakandakare-Maia, E.T.; Siqueira, J.S.; Ferron, A.J.T.; Vieira, T.A.; Palacio, T.L.N.; Grandini, N.A.; Garcia, J.L.; Belin, M.A.; Altomare, A.; Baron, G.; et al. Treatment with Bergamot (*Citrus bergamia*) Leaves Extract Attenuates Leptin Resistance in Obese Rats. *Mol. Cell. Endocrinol.* **2023**, *566*, 111908. [CrossRef] [PubMed]
22. Palacio, T.L.N.; Siqueira, J.S.; de Paula, B.H.; Rego, R.M.P.; Vieira, T.A.; Baron, G.; Altomare, A.; Ferron, A.J.T.; Aldini, G.; Kano, H.T.; et al. Bergamot (*Citrus bergamia*) Leaf Extract Improves Metabolic, Antioxidant and Anti-Inflammatory Activity in Skeletal Muscles in a Metabolic Syndrome Experimental Model. *Int. J. Food Sci. Nutr.* **2023**, *74*, 64–71. [CrossRef] [PubMed]
23. Gonc, D.F.; Paola, B.; Rafacho, M.; Assis, B.; Jaldin, G.; Bruder, T.; Alves, M.; Silva, B.; Antonio, L.; Zornoff, M.; et al. Vitamin D Induces Increased Systolic Arterial Pressure via Vascular Reactivity and Mechanical Properties. *PLoS ONE* **2014**, *9*, e98895. [CrossRef]
24. Matthews, D.R.; Hosker, J.P.; Rudenski, A.S.; Naylor, B.A.; Treacher, D.F.T.R.; Matthews, D.R.; Hosker, J.P.; Rudenski, A.S.; Naylor, B.A.; Treacher, D.F.; et al. Homeostasis Model Assessment: Insulin Resistance and Beta-Cell Function from Fasting Plasma Glucose and Insulin Concentrations in Man. *Diabetologia* **1985**, *28*, 412–419. [CrossRef]
25. Moreto, F.; Ferron, A.J.T.; Francisqueti-Ferron, F.V.; D'Amato, A.; Garcia, J.L.; Costa, M.R.; Silva, C.C.V.A.; Altomare, A.; Correa, C.R.; Aldini, G.; et al. Differentially Expressed Proteins Obtained by Label-free Quantitative Proteomic Analysis Reveal Affected Biological Processes and Functions in Western Diet-induced Steatohepatitis. *J. Biochem. Mol. Toxicol.* **2021**, *35*, 1–11. [CrossRef]
26. Giannini, E.G. Liver Enzyme Alteration: A Guide for Clinicians. *Can. Med. Assoc. J.* **2005**, *172*, 367–379. [CrossRef]
27. Francisqueti, F.V.; Ferron, A.J.T.; Hasimoto, F.K.; Alves, P.H.R.; Garcia, J.L.; Santos, K.C.; Moreto, F.; Ferreira, A.L.A.; Minatel, I.O.; Corrêa, C.R. Gamma Oryzanol Treats Obesity-Induced Kidney Injuries by Modulating the Adiponectin Receptor 2 / PPAR-α Axis. *Oxid. Med. Cell. Longev.* **2018**, *2018*, 1278392. [CrossRef]
28. Mesquita, C.S.; Oliveira, R.; Bento, F.; Geraldo, D.; Rodrigues, J.V.; Marcos, J.C. Simplified 2,4-Dinitrophenylhydrazine Spectrophotometric Assay for Quantification of Carbonyls in Oxidized Proteins. *Anal. Biochem.* **2014**, *458*, 69–71. [CrossRef]
29. Marklund, S.L. Product of Extracellular-Superoxide Dismutase Catalysis. *FEBS Lett.* **1985**, *184*, 237–239. [CrossRef]
30. Aebi, H. Catalase. In *Methods of Enzymatic Analysis*; Elsevier: Amsterdam, The Netherlands, 1974; pp. 673–684.

31. Benzie, I.F.F.; Strain, J.J. The Ferric Reducing Ability of Plasma (FRAP) as a Measure of "Antioxidant Power": The FRAP Assay. *Anal. Biochem.* **1996**, *239*, 70–76. [CrossRef]
32. Rodríguez-Correa, E.; González-Pérez, I.; Clavel-Pérez, P.I.; Contreras-Vargas, Y.; Carvajal, K. Biochemical and Nutritional Overview of Diet-Induced Metabolic Syndrome Models in Rats: What Is the Best Choice? *Nutr. Diabetes* **2020**, *10*, 24. [CrossRef] [PubMed]
33. Ferrari, F.; Bock, P.M.; Motta, M.T.; Helal, L. Biochemical and Molecular Mechanisms of Glucose Uptake Stimulated by Physical Exercise in Insulin Resistance State: Role of Inflammation. *Arq. Bras. Cardiol.* **2019**, *113*, 1139–1148. [CrossRef]
34. Kalra, A.; Yetiskul, E.; Wehrle, C.J.; Tuma, F. *Physiology, Liver*; StatPearls Publishing: Treasure Island, FL, USA, 2023.
35. Corless, J.K. Normal Liver Function. A Basis for Understanding Hepatic Disease. *Arch. Intern. Med.* **1983**, *143*, 2291–2294. [CrossRef] [PubMed]
36. Rives, C.; Fougerat, A.; Ellero-Simatos, S.; Loiseau, N.; Guillou, H.; Gamet-Payrastre, L.; Wahli, W. Oxidative Stress in NAFLD: Role of Nutrients and Food Contaminants. *Biomolecules* **2020**, *10*, 1702. [CrossRef]
37. Pafili, K.; Roden, M. Nonalcoholic Fatty Liver Disease (NAFLD) from Pathogenesis to Treatment Concepts in Humans. *Mol. Metab.* **2021**, *50*, 101122. [CrossRef] [PubMed]
38. Ren, B.; Qin, W.; Wu, F.; Wang, S.; Pan, C.; Wang, L.; Zeng, B.; Ma, S.; Liang, J. Apigenin and Naringenin Regulate Glucose and Lipid Metabolism, and Ameliorate Vascular Dysfunction in Type 2 Diabetic Rats. *Eur. J. Pharmacol.* **2016**, *773*, 13–23. [CrossRef]
39. Aboulaghras, S.; Sahib, N.; Bakrim, S.; Benali, T.; Charfi, S.; Guaouguaou, F.-E.; Omari, N.E.; Gallo, M.; Montesano, D.; Zengin, G.; et al. Health Benefits and Pharmacological Aspects of Chrysoeriol. *Pharmaceuticals* **2022**, *15*, 973. [CrossRef]
40. Punithavathi, V.R.; Anuthama, R.; Prince, P.S.M. Combined Treatment with Naringin and Vitamin C Ameliorates Streptozotocin-Induced Diabetes in Male Wistar Rats. *J. Appl. Toxicol.* **2008**, *28*, 806–813. [CrossRef]
41. Kawser Hossain, M.; Abdal Dayem, A.; Han, J.; Yin, Y.; Kim, K.; Kumar Saha, S.; Yang, G.-M.; Choi, H.; Cho, S.-G. Molecular Mechanisms of the Anti-Obesity and Anti-Diabetic Properties of Flavonoids. *Int. J. Mol. Sci.* **2016**, *17*, 569. [CrossRef]
42. Mirarchi, A.; Mare, R.; Musolino, V.; Nucera, S.; Mollace, V.; Pujia, A.; Montalcini, T.; Romeo, S.; Maurotti, S. Bergamot Polyphenol Extract Reduces Hepatocyte Neutral Fat by Increasing Beta-Oxidation. *Nutrients* **2022**, *14*, 3434. [CrossRef]
43. Cha, J.Y.; Cho, Y.S.; Kim, I.; Anno, T.; Rahman, S.M.; Yanagita, T. Effect of Hesperetin, a Citrus Flavonoid, on the Liver Triacylglycerol Content and Phosphatidate Phosphohydrolase Activity in Orotic Acid-Fed Rats. *Plant Foods Hum. Nutr.* **2001**, *56*, 349–358. [CrossRef] [PubMed]
44. Carresi, C.; Gliozzi, M.; Musolino, V.; Scicchitano, M.; Scarano, F.; Bosco, F.; Nucera, S.; Maiuolo, J.; Macrì, R.; Ruga, S.; et al. The Effect of Natural Antioxidants in the Development of Metabolic Syndrome: Focus on Bergamot Polyphenolic Fraction. *Nutrients* **2020**, *12*, 1504. [CrossRef] [PubMed]
45. Musolino, V.; Gliozzi, M.; Scarano, F.; Bosco, F.; Scicchitano, M.; Nucera, S.; Carresi, C.; Ruga, S.; Zito, M.C.; Maiuolo, J.; et al. Bergamot Polyphenols Improve Dyslipidemia and Pathophysiological Features in a Mouse Model of Non-Alcoholic Fatty Liver Disease. *Sci. Rep.* **2020**, *10*, 2565. [CrossRef] [PubMed]
46. Salehi, B.; Venditti, A.; Sharifi-Rad, M.; Kręgiel, D.; Sharifi-Rad, J.; Durazzo, A.; Lucarini, M.; Santini, A.; Souto, E.; Novellino, E.; et al. The Therapeutic Potential of Apigenin. *Int. J. Mol. Sci.* **2019**, *20*, 1305. [CrossRef] [PubMed]
47. Paredes-Gonzalez, X.; Fuentes, F.; Jeffery, S.; Saw, C.L.-L.; Shu, L.; Su, Z.-Y.; Kong, A.-N.T. Induction of NRF2-Mediated Gene Expression by Dietary Phytochemical Flavones Apigenin and Luteolin. *Biopharm. Drug Dispos.* **2015**, *36*, 440–451. [CrossRef]
48. Parafati, M.; Lascala, A.; La Russa, D.; Mignogna, C.; Trimboli, F.; Morittu, V.; Riillo, C.; Macirella, R.; Mollace, V.; Brunelli, E.; et al. Bergamot Polyphenols Boost Therapeutic Effects of the Diet on Non-Alcoholic Steatohepatitis (NASH) Induced by "Junk Food": Evidence for Anti-Inflammatory Activity. *Nutrients* **2018**, *10*, 1604. [CrossRef]
49. Oguntibeju, O.O. Type 2 Diabetes Mellitus, Oxidative Stress and Inflammation: Examining the Links. *Int. J. Physiol. Pathophysiol. Pharmacol.* **2019**, *11*, 45–63.